 DOI: 10.1002/masy.200951102

Simulation of Propylene Polymerization in Industrial Reactors Using Ziegler-Natta Catalysts in the Presence of Electron Donors

*Ahmad Alshaiban, João B. P. Soares**

Summary: Heterogeneous Ziegler-Natta catalysts are still the most important catalysts for the industrial production of polyolefins, despite the discovery of high-activity metallocene systems in the eighties. Despite of their huge commercial importance, several aspects of Ziegler-Natta catalysts are still poorly understood from both qualitative and quantitative points of view. Especially for polypropylene, a very important factor controlling product quality is the effect of the electron donor used to modify the catalyst. In this manuscript we present, for the first time, a quantitative mathematical model that describes the effect of electron donors on the tacticity of polypropylene made with multiple-site type catalysts.

Keywords: electron donor; mathematical modeling; polypropylene; simulation; Ziegler-Natta catalyst

Introduction

Heterogeneous Ziegler-Natta catalysts are responsible for most of the industrial production of polyethylene and polypropylene. A unique feature of these catalysts is the presence of more than one active site type, leading to the production of polyolefins with broad distributions of molecular weight (MWD), chemical composition (CCD) and stereoregularity. These distributions influence strongly the mechanical and rheological properties of polyolefins and are ultimately responsible for the performance and final applications of the product.[1–3]

Despite being used industrially for almost half a century, the nature of active sites on heterogeneous Ziegler-Natta catalysts is still not well understood. Their inherent complexity, where mass and heat transfer limitations are combined with a rather complex chemistry of site activation in the presence of internal and external donors, plus other phenomena such as comonomer rate enhancement, hydrogen effects, and poisoning, makes their quantitative description very challenging. Because of this complexity, the production of polyolefins with controlled microstructures using Ziegler-Natta catalysts has been much harder to attain than with single-site catalysts such as metallocenes.[4]

In this manuscript, we developed mathematical models for the steady-state and dynamic simulation of propylene polymerization using Ziegler-Natta reactors. Two different modeling techniques were compared (population balances/method of moments, and Monte Carlo simulation) and a new mechanistic step (site transformation by electron donors) were simulated for the first time.

Model Development

The tacticity distribution of polypropylene is one of its most important properties and it can be significantly altered by the use of internal and external electron donors.[5] However, no detailed mathematical model has been developed to date to describe the

Department of Chemical Engineering, University of Waterloo, 200 University Avenue West, Waterloo, Ontario, Canada N2L 3G1
E-mail: jsoares@uwaterloo.ca

Copyright © 2009 WILEY-VCH Verlag GmbH & Co. KGaA, Weinheim

influence of electron donors on the tacticity distribution of polypropylene made with multiple-site catalysts. We may postulate the existence of at least three types of active sites on Ziegler-Natta catalysts used for propylene polymerization: sites that make only atactic chains, sites that make only isotactic chains, and sites that may alternate between stereoselective and aspecific states. Based on the mechanistic studies of Kakugo *et al.*[6] and Busico *et al.*,[7,8] atactic sites can be reversibly converted to isotactic sites by complexation with an electron donor molecule. Therefore, these sites can exist under two states, atactic or isotactic. If this conversion takes place during the lifetime of a polypropylene chain, stereoblock chains (atactic-isotactic-atactic-isotactic-...) may be formed.

The active site type that can alternate between stereospecific and aspecific states can produce three types of dead polymer chains: 1) purely isotactic chains that are formed when they grow during the stereospecific state and terminate before transformation to the atactic state, 2) purely atactic chains that are formed when they grow during the aspecific state and terminate before transformation to the stereospecific state, and 3) stereoblock chains that are formed when the site state changes from stereospecific to aspecific and/or vice-versa during the life time of the chain. Stereoblock chains can be further subdivided into diblock, triblock, tetrablock, and higher multiblock chains as shown in Figure 1. The whole population can be also subdivided into overall atactic and isotactic segments as illustrated in Figure 1.

According to Busico *et al.*,[7] the reversible transformation from stereospecific to aspecific state may happen during chain growth. Based on this mechanism, we proposed polymerization kinetic steps for active sites that can assume stereospecific (*I*) and aspecific (*II*) states as expressed in Table 1, Equations (5) to (10). For instance, Equation (7) shows how the living chain $P^{II}_{r,i}$ at state *II* (with length *r* and *i* stereoblocks) undergoes a site transformation to state *I* by complexation with donor *Do*, increasing its numbers of stereoblocks to $i+1$ and maintaining the same chain length *r* ($P^{I}_{r,i+1}$). The reverse step is given in Equation (8). Other steps included in the reaction mechanism shown in Table 1 are: site activation, chain initiation, propagation, chain transfer, site deactivation, and catalyst poisoning.[9]

Population Balances and the Method of Moments

We formulated three population balances to monitor different microstructural properties of the polypropylene chains: 1) balances for the whole chains, without monitoring the number or type of stereoblocks per chain; 2) balances for purely isotactic, purely atactic, and stereoblock chains; and 3) balances for chain segments (Equations (9) and (10)). Moment

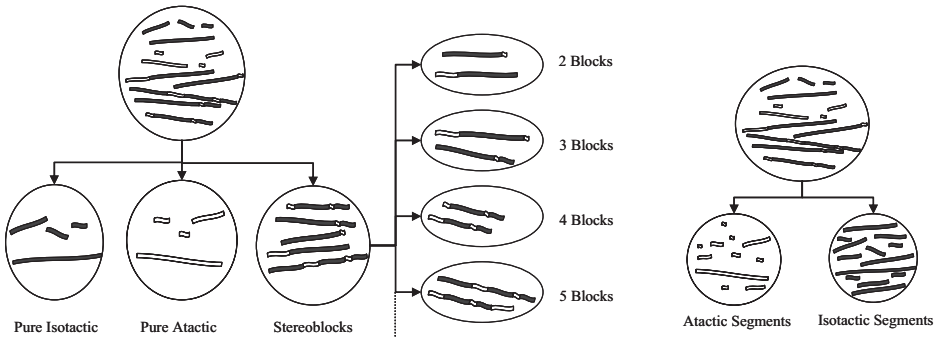

Figure 1.
Chain populations with different number of stereoblocks (whole chains) and chain length distributions for chain segments.

Copyright © 2009 WILEY-VCH Verlag GmbH & Co. KGaA, Weinheim

Table 1.
Elementary steps of the polymerization mechanism ($j = I$ or II, and $P^j_{C*} = P^j_0, P^j_H$, or P^j_{Et}).[9]

Step	Equation	#	Step	Equation	#
Activation	$C_j + Al \xrightarrow{k^j_a} P^j_0$	(1)	Propagation	$P^j_{r,i} + M \xrightarrow{k^j_p} P^j_{r+1,i}$	(11)
Initiation	$P^j_0 + M \xrightarrow{k^j_i} P^j_{1,1}$	(2)	Termination by:		
	$P^j_H + M \xrightarrow{k^j_{iH}} P^j_{1,1}$	(3)	β-hydride elimination	$P^j_{r,i} \xrightarrow{k^j_\beta} P^j_H + D^j_{r,i}$	(12)
	$P^j_{Et} + M \xrightarrow{k^j_{iR}} P^j_{1,1}$	(4)	Hydrogen	$P^j_{r,i} + H_2 \xrightarrow{k^j_H} P^j_H + D^j_{r,i}$	(13)
Transformation by Donor			Monomer	$P^j_{r,i} + M \xrightarrow{k^j_M} P^j_{1,1} + D^j_{r,i}$	(14)
	$P^{II}_{C*} + Do \xrightarrow{k^+_{Do}} P^I_{C*}$	(5)	Aluminum	$P^j_{r,i} + Al \xrightarrow{k^j_{Al}} P^j_{Et} + D^j_{r,i}$	(15)
	$P^I_{C*} \xrightarrow{k^-_{Do}} P^{II}_{C*} + Do$	(6)	Deactivation	$P^j_{r,i} \xrightarrow{k^j_d} C_d + D^j_{r,i}$	(16)
	$P^{II}_{r,i} + Do \xrightarrow{k^+_{Do}} P^I_{r,i+1}$	(7)	Poisoning	$P^j_{r,i} + I \xrightarrow{k^j_{d\text{-}I}} C_d + D^j_{r,i}$	(17)
	$P^I_{r,i} \xrightarrow{k^-_{Do}} P^{II}_{r,i+1} + Do$	(8)			
	$P^{II}_{r,i} + Do \xrightarrow{k^+_{Do}} B^{II}_r + P^I_{0,i+1}$	(9)			
	$P^I_{r,i} \xrightarrow{k^-_{Do}} B^I_r + P^{II}_{0,i+1} + Do$	(10)			

equations were then developed based on these population balances.

The population balances shown in Appendix A (Tables A-1 and A-2) encompass thousands of equations, one for each polymer of a given chain length r. (The derived balances describe only the polymerization taking place in active sites that can undergo the stereospecific-aspecific transition discussed above. Active sites that produce only isotactic or atactic chains are much easier to model, since their behavior is a particular solution (when no site transition takes place) of the general model.) Even though mathematical methods exist to solve these very large systems of differential equations,[10] the method of moments can be used to reduce the number of equations required in the simulation.[11,12] The moments of the living and dead chains for the whole chains are defined by Equations (18) and (19), respectively, where $j = I$ or II represent the site state, and m is the moment order. The zeroth moment, defined when $m = 0$, measures the total number of polymer moles in a given population. The first moment, $m = 1$, is the total mass of the polymer population. Finally, the second moment, $m = 2$, does not have physical meaning but is required to calculate the weight average molecular weight.

The method of moments can be used to estimate the number (M_n) and weight (M_w) average molecular weights of the polymer populations as expressed in Equations (20) and (21), where mw is the molar mass of the repeating unit ($mw = 42$ g/mol for propylene). Finally, the polydispersity index is easily calculated as shown in Equation (22). The number and weight average molecular weights (M_n and M_w) for each individual species (i.e. pure isotactic chains) are calculated using expressions similar to Equations (20) and (21) using their respective moments. Moreover, the molar and mass fractions of isotactic chains can be calculated using the moments of each individual species as illustrated in Equations (23) and (24), respectively. Moment equations for chain segments were derived in a similar way. The moments for the isotactic or atactic ($j = I$ or II) segments are defined in Equation (25). For instance, the number and weight average molecular weights of the isotactic segments (when $j = I$) can be calculated with Equations (26) and (27) respectively and their polydispersity is given by Equation (28). The number and weight average molecular weights of

Copyright © 2009 WILEY-VCH Verlag GmbH & Co. KGaA, Weinheim

Table 2.
Moments general formulation, molecular weight equations, and tacticity percentage calculation.

$Y_j^m = \sum_{r=1}^{\infty} r^m P_r^j$	(18)	$\text{Purely isotactic mass\%} = \frac{X_{I,1}^1 + Y_{I,1}^1}{X_I^1 + Y_I^1 + X_{II}^1 + Y_{II}^1} \times 100$	(24)
$X_j^m = \sum_{r=1}^{\infty} r^m D_r^j$	(19)	$W_j^m = \sum_{r=1}^{\infty} r^m B_r^j$	(25)
$M_n = mw.\frac{\sum_{r=1}^{\infty} rN_r}{\sum_{r=1}^{\infty} N_r} = mw.\frac{X_I^1 + Y_I^1 + X_{II}^1 + Y_{II}^1}{X_I^0 + Y_I^0 + X_{II}^0 + Y_{II}^0}$	(20)	$\overline{M}_n^j = mw.\frac{W_j^1}{W_j^0}$	(26)
$M_w = mw.\frac{\sum_{r=1}^{\infty} r^2 N_r}{\sum_{r=1}^{\infty} rN_r} = mw.\frac{X_I^2 + Y_I^2 + X_{II}^2 + Y_{II}^2}{X_I^1 + Y_I^1 + X_{II}^1 + Y_{II}^1}$	(21)	$\overline{M}_w^j = mw.\frac{W_j^2}{W_j^1}$	(27)
$PDI = M_w / M_n$	(22)	$PDI_s^j = \overline{M}_w^j / \overline{M}_n^j$	(28)
$\text{Purely isotactic mole\%} = \frac{X_{I,1}^0 + Y_{I,1}^0}{X_I^0 + Y_I^0 + X_{II}^0 + Y_{II}^0} \times 100$	(23)		

the atactic segments are calculated with the same equations when $j = II$.

Monte Carlo Simulation

Monte Carlo simulation uses randomly generated numbers to select one event from a series of events based on its probability of occurrence. For our model of olefin polymerization, probabilities can be defined for propagation, termination, and site transformation. Since the chains are simulated one-by-one, the maximum microstructural information can be obtained by Monte Carlo simulation. In olefin polymerization, several researchers have used Monte Carlo simulation to keep track of microstructural information that could not be achieved by other modeling techniques. Simon and Soares [13] used a Monte Carlo model to describe the long-chain branch formation in polyethylene made with a combination of single-site catalysts. A Monte Carlo model was also used to analyze the microstructure of polyolefin thermoplastic elastomers made with two single-site catalysts.[14] Beigzadeh *et al.*[15] simulated CRYSTAF fractionation of ethylene/1-octene copolymers made with single-site catalysts using a Monte Carlo model.

In this work, we used Monte Carlo techniques to develop a model to simulate propylene polymerization taking in consideration site transformation in the presence of electron donors. The model can predict the same properties modeled by the method of moments and, in addition, the complete MWD of the several polymer populations. Figure 2 shows the algorithm developed for the one-site, two-state catalyst model proposed in Table 1. The model consists of two main loops: one for constructing the isotactic segments (growing when the site is in the isospecific state) and the other for constructing the atactic segments (when the site is in the aspecific state). In each loop, a propagation, termination, or state transformation event may take place. The probabilities of each event have been calculated using the values of the rate of reaction equations as expressed in Table 3, where R_p is the rate of propagation, R_{tr} is the overall chain transfer rate, $R_{tf,I}$ is rate of site transformation of state I to II, $R_{tf,II}$ is the rate of site transformation from state II to I, and $j = I$ or II for site states. As shown in Figure 2, the algorithm starts by generating a random number (*Rand*), uniformly distributed between zero and one, which is then used to select a reaction step. The algorithm generally starts with the site in the most probable state, the isospecific state I, but the choice of initial state will not affect the outcome of the simulations. The probability for each event taking place is given by the ratio of the rate for that event divided by the sum of the rates of all events, as shown in Equations (33) to (35), where P_{pj} is the probability of propagation, P_{trj} is the probability of termination, and P_{tfj} is the probability of transformation at state $j = I$ or II.

Results and Discussions

In this section, we will compare the steady-state solutions for the method of moments and Monte Carlo solutions. First, the steady-state solution for a single-site catalyst (assuming states I or II) was used to

Copyright © 2009 WILEY-VCH Verlag GmbH & Co. KGaA, Weinheim

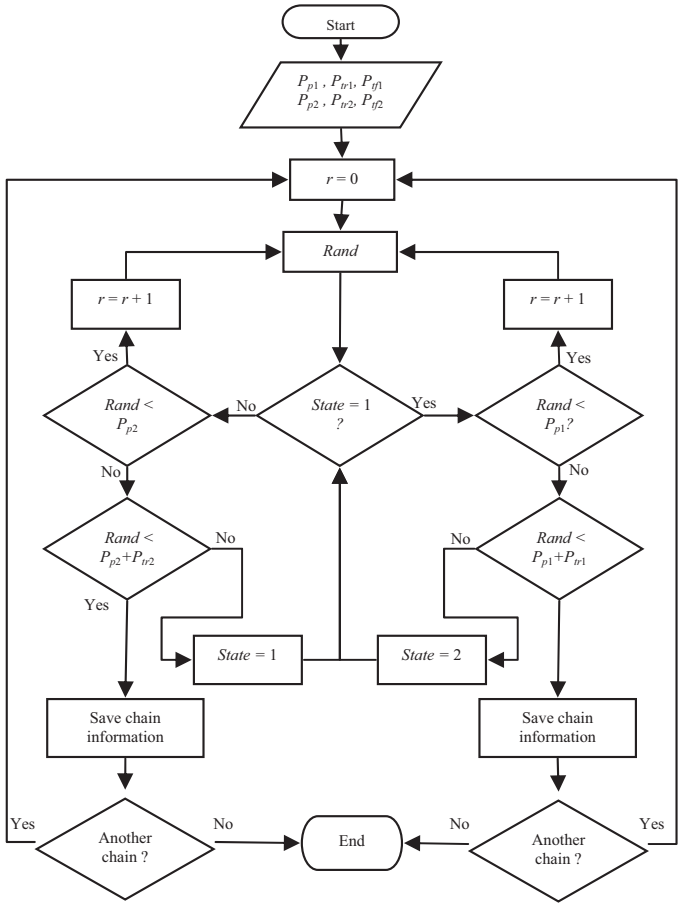

Figure 2.
Monte Carlo simulation flowchart.

Table 3.
Reaction rate equations and Monte Carlo probabilities.

$R_{pj} = k_p^j M P_r^j$	(29)	$P_{pj} = R_{pj}/\{R_{pj} + R_{trj} + R_{tfj}\}$	(33)
$R_{tr,j} = (K_{T,j} + K_{D,j}) P_r^j$	(30)	$P_{trj} = R_{trj}/\{R_{pj} + R_{trj} + R_{tfj}\}$	(34)
$R_{tf,I} = k_{Do}^{-} P_r^j$	(31)	$P_{tfj} = R_{tfj}/\{R_{pj} + R_{trj} + R_{tfj}\}$	(35)
$R_{tf,II} = k_{Do}^{+} DoP_r^{II}$	(32)		

simulate the polymerization of propylene in a CSTR at different operating conditions. The effect of donor, hydrogen, and monomer concentrations on polypropylene microstructure were investigated. Moreover, the effect of changing the values of some kinetic parameters on the microstructure of polypropylene was also studied. Finally, the model was extended to include a total of four site types, which represents the situation more commonly encountered with heterogeneous Ziegler-Natta catalysts. In addition to steady-state simulations, the dynamic behavior of propylene polymerization in a CSTR with a single-site and a four-site type catalyst were also simulated, but will not be shown herein.[9]

Table 4 lists the concentrations of catalyst, cocatalyst, electron donor, propylene and other reagents under the reference simulation conditions.

Copyright © 2009 WILEY-VCH Verlag GmbH & Co. KGaA, Weinheim

Table 4.
Reference polymerization conditions.

	mol/L		mol/L
C_I	0.00001	*Al*	0.0007
C_{II}	0.00001	*I*	0
M	0.20	H_2	0.004
Do	0.0007		

Table 5 shows the reference values for the reaction kinetic rate constants used in the simulations. Unless otherwise stated, these were the conditions used in all simulations.

Simulations with the Method of Moments

The moment equations can be solved analytically at steady-state, as shown in Table 6 and Table A-3, as derived by Alshaiban.[9] The model was first solved for one single site type with two states, stereospecific (making isotactic chains or blocks) and aspecific (producing atactic chains or blocks). We believe these simulations represent the main contribution of this paper, since no mathematical model for active sites existing in two states has been presented in the literature, even though the concept has been analyzed qualitatively in many previous publications, as discussed above.

The following discussion summarizes the responses to changes in donor type and concentration and hydrogen concentration. Figure 3 shows that, in the absence of electron donor, no stereoblock chains are made, only purely atactic or isotactic chains. This is, of course, a consequence of our choice of model parameters in Table 1: the concentration of active sites fed to the reactor in state *I* and *II* is the same and they have the same value for their propagation rate constants; consequently, in the absence of electron donors, no site transformation will take place and both states will make the same amount of polymer. Contrarily, when electron donor is introduced in the reactor, a significant

Table 5.
Reference reaction rate constants ($j = I$ or II for site states).

Constant	(L/mol·s)	Constant	(L/mol·s)	Constant	(s^{-1})
k^j_a	3,000	k^+_{Do}	150	k_{Do^-}	0.01
k^j_i	3,000	k^j_{Al}	0	k^j_β	0
k^j_p	3,000	$k_{Al\text{-}I}$	10,000	k^j_d	0.001
k^j_H	110	k^j_M	0		
$k^j_{d\text{-}I}$	8,000				

Table 6.
Moments equations at steady state (refer to Table A- 3 for the active species equations and term definitions).

	State *I* (Isotactic)	#	State *II* (Atactic)	#
Overall	$Y^0_I = \gamma'_1 M + \beta'_1 Y^0_{II}$	(36)	$Y^0_{II} = \gamma'_2 M + \beta'_2 Y^0_I$	(40)
	$Y^1_I = \gamma'_1 M + \delta'_1 M Y^0_I + \beta'_1 Y^1_{II}$	(37)	$Y^1_{II} = \gamma'_2 M + \delta'_2 M Y^0_{II} + \beta'_2 Y^1_I$	(41)
	$Y^2_I = \gamma'_1 M + \delta'_1 M(2Y^1_I + Y^0_I) + \beta'_1 Y^2_{II}$	(38)	$Y^2_{II} = \gamma'_2 M + \delta'_2 M(2Y^1_{II} + Y^0_{II}) + \beta'_2 Y^2_I$	(42)
	$X^m_I = (1/s)(K_{T1} + K_{D1}) Y^m_I$	(39)	$X^m_{II} = (1/s)(K_{T2} + K_{D2}) Y^m_{II}$	(43)
Pure Polymer ($i = 1$)	$Y^0_{I,1} = \gamma_1 M + \delta''_1 M Y^0_I$	(44)	$Y^0_{II,1} = \gamma_2 M + \delta''_2 M Y^0_{II}$	(48)
	$Y^1_{I,1} = \gamma_1 M + \delta_1 M Y^0_{I,1} + \delta''_1 M Y^1_I$	(45)	$Y^1_{II,1} = \gamma_2 M + \delta_2 M Y^0_{II,1} + \delta''_2 M Y^1_{II}$	(49)
	$Y^2_{I,1} = \gamma_1 M + \delta_1 M(2Y^1_{I,1} + Y^0_{I,1}) + \delta''_1 M Y^2_I$	(46)	$Y^2_{II,1} = \gamma_2 M + \delta_2 M(2Y^1_{II,1} + Y^0_{II,1}) + \delta''_2 M Y^2_{II}$	(50)
	$X^m_{I,1} = (1/s)(K_{T1} + K_{D1}) Y^m_{I,1}$	(47)	$X^m_{II,1} = (1/s)(K_{T2} + K_{D2}) Y^m_{II,1}$	(51)
Stereoblocks ($i > 1$)	$Y^0_{I,i} = \beta_1 Y^0_{II,i-1}$	(52)	$Y^0_{II,i} = \beta_2 Y^0_{I,i-1}$	(56)
	$Y^1_{I,i} = \delta_1 M Y^0_{I,i} + \beta_1 Y^1_{II,i-1}$	(53)	$Y^1_{II,i} = \delta_2 M Y^0_{II,i} + \beta_2 Y^1_{I,i-1}$	(57)
	$Y^2_{I,i} = \delta_1 M(2Y^1_{I,i} + Y^0_{I,i}) + \beta_1 Y^2_{II,i-1}$	(54)	$Y^2_{II,i} = \delta_2 M(2Y^1_{II,i} + Y^0_{II,i}) + \beta_2 Y^2_{I,i-1}$	(58)
	$X^m_{I,i} = (1/s)(K_{T1} + K_{D1}) Y^m_{I,i}$	(55)	$X^m_{II,i} = (1/s)(K_{T2} + K_{D2}) Y^m_{II,i}$	(59)
Segments	$W^0_I = \gamma''_1 M$	(60)	$W^0_{II} = \gamma''_2 M$	(63)
	$W^1_I = \gamma''_1 M + \delta_1 M W^0_I$	(61)	$W^1_{II} = \gamma''_2 M + \delta_2 M W^0_{II}$	(64)
	$W^2_I = \gamma''_1 M + \delta_1 M(2W^1_I + W^0_I)$	(62)	$W^2_{II} = \gamma''_2 M + \delta_2 M(2W^1_{II} + W^0_{II})$	(65)

Copyright © 2009 WILEY-VCH Verlag GmbH & Co. KGaA, Weinheim

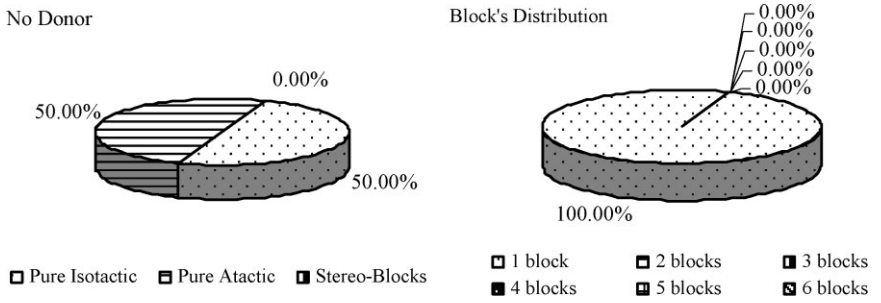

Figure 3.
Tacticity and block distributions for propylene made with a single-site catalyst without donor at the reference polymerization conditions. ($k_p^I/k_p^{II} = 1$, $R_p^I/R_{tr}^I = 1364$, $R_p^{II}/R_{tr}^{II} = 1364$, $M_n = 57{,}250$ g/mol, $M_w = 114{,}500$ g/mol, and $PDI = 2.00$).

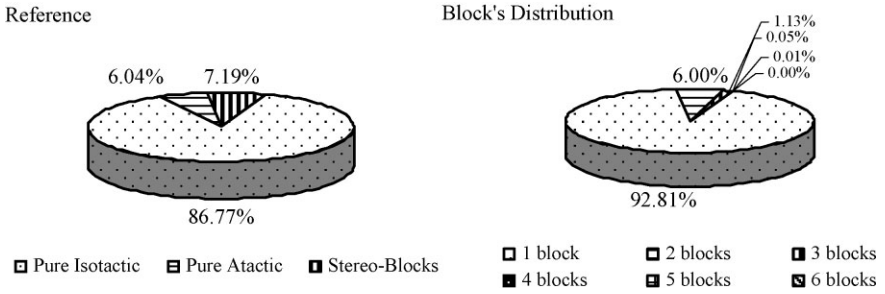

Figure 4.
Tacticity and block distributions for propylene made with a single-site catalyst at reference polymerization conditions. ($k_p^I/k_p^{II} = 1$, $R_p^I/R_{tr}^I = 1364$, $R_p^{II}/R_{tr}^{II} = 1364$, $M_n = 57{,}250$ g/mol, $M_w = 114{,}500$ g/mol, and $PDI = 2.00$).

fraction of sites on state *II* (aspecific) are converted to state *I* (isospecific), decreasing the mass fraction of atactic polypropylene to approximately 6%, with the consequent increase in the fraction of isotactic and stereoblock chains to about 87% and 7%, respectively, as illustrated in Figure 4. Interestingly, according to the simulations, most of the stereoblock chains are atactic-isotactic diblocks (6%), with a very low fraction of multiblock chains (1%).

The effect of changing donor concentration is illustrated in Figure 5, where it is reduced by half of the value used in the simulations shown in Figure 4; the mass fraction of atactic polypropylene increases from 6.04% to 13.38%, as expected. Contrarily, when the donor concentration is

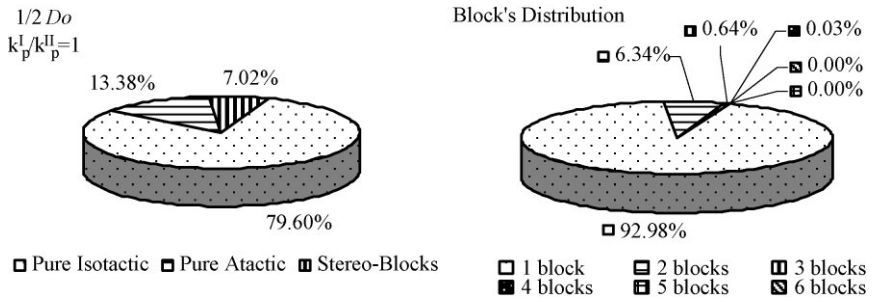

Figure 5.
Tacticity and block distributions for propylene made with a single-site catalyst with half the reference donor concentration shown in Figure 4. Other polymerization conditions are the same as shown in Figure 4.

Copyright © 2009 WILEY-VCH Verlag GmbH & Co. KGaA, Weinheim

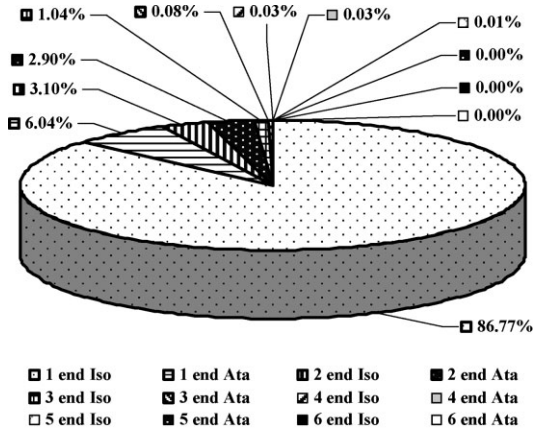

Figure 6.
Mass fractions of stereoblock chain populations for the reference polymerization conditions shown in Table 4.

doubled, the mass fraction of atactic polypropylene will be reduced to 2.26%. The mass fraction of stereoblock chains is also affected by the concentration of electron donor, but the diblock chains continue to be the dominant population among the stereoblock chains for all simulations.

Figure 6 shows the complete weight distribution for the stereoblock chains, and Table 7 their molecular weight averages (M_n, M_w, and *PDI*). We have also classified the chains according to the state of the site when chain growth was terminated. This distinction is immaterial for the case of diblocks, but is important for triblocks and higher odd-numbered multiblock chains, since an isotactic-terminated chain (isotactic-atactic-isotactic-...) has a different microstructure from an atactic-terminated chain (atactic-isotactic-atactic-...) for odd-numbered multiblock chains. Table 7 shows that the molecular weight averages increase and the polydispersity index decreases with increasing number of blocks per chain. Both trends are expected, since longer chains will have a higher probability of experiencing site transformation events than shorter chains; the effect on *PDI* is a simple consequence of sampling an increasingly narrower polymer population: uniblock chains are those that follow Flory's statistics with $PDI = 2$, diblocks will have $PDI = 1.5$ in a similar fashion to chains made by termination by combination in free radical polymerization, and chains with three or more blocks will have even narrower MWDs, since they are being selected from a subpopulation with increasing molecular weights.

Figure 7 shows the effect of changing the relative propagation rates of states *I* and *II*. The value of k_p^I/k_p^{II} has been increased to 10, as opposed to Figure 4 where $k_p^I/k_p^{II} = 1$. As expected, the fraction of

Table 7.
Molecular weight averages and polydispersity for stereoblock chains made under the reference polymerization conditions.

# of blocks	End with isotactic block			End with atactic block		
i	M_n	M_w	*PDI*	M_n	M_w	*PDI*
1	56,000	112,000	2.00	46,250	92,500	2.00
2	102,230	153,800	1.50	102,230	153,800	1.50
3	158,200	211,330	1.34	148,500	198,400	1.34
4	204,400	256,000	1.25	204,400	256,000	1.25
5	260,350	312,900	1.20	250,600	301,200	1.20
6	306,600	358,200	1.17	306,600	358,200	1.17

Copyright © 2009 WILEY-VCH Verlag GmbH & Co. KGaA, Weinheim

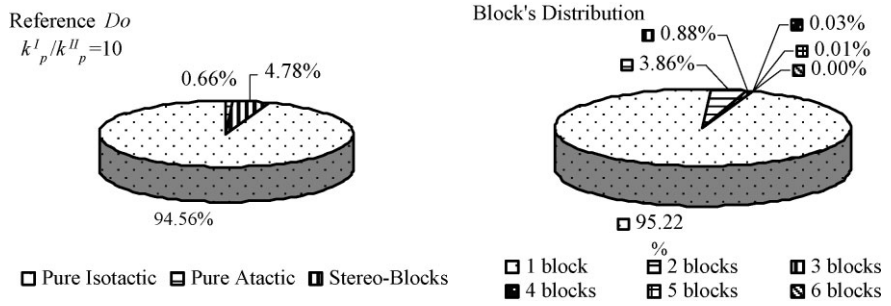

Figure 7.
Tacticity and block distributions for propylene made with a single-site catalyst at normal donor concentration and increased k^I_p/k^{II}_p ratio ($k^I_p/k^{II}_p = 10$, $R^I_p/R^I_{tr} = 1364$, $R^{II}_p/R^{II}_{tr} = 136$, $M_n = 52{,}600$ g/mol, $M_w = 111{,}800$ g/mol, $PDI = 2.13$).

purely atactic chains drops from approximately 6% to 0.66% as the ratio k^I_p/k^{II}_p increases, since much more polymer is made during state *I* in this case. In addition, since the two states produce polymer with different molecular weight averages, a broadening of the MWD will take place and *PDI* is higher than 2. In the previous simulations we assumed that both states produced polypropylene with the same average molecular weights.

The effect of donor type has been also examined by manipulating the values of the parameter for site transformation by donor, k^+_{Do} and k^-_{Do}. Figure 8 shows the effect of selecting donor types with different values of site transformation rate constants. When the value of k^+_{Do} is doubled and k^-_{Do} is reduced by a factor of $1/2$ with respect with the value listed in Table 4, the mass fraction of purely isotactic chain increases to 95.07% (as compared to 86.77% for the reference case) as shown in Figure 8. No significant effect is observed in the values of M_n, M_w, and *PDI*, since the propagation and termination rates are not affected by site state transformation. The use of better donors also reduces the weight percent of stereoblock chains, since the transition from isotactic to atactic state is less likely to occur during the lifetime of a polypropylene chain.

Figure 9 studies the effect of changing the concentration of hydrogen on polypropylene microstructure. Molecular weight naturally decreases with increasing hydrogen concentration. More interesting, changes in hydrogen concentration also have a pronounced effect on the fraction of stereoblock chains. This may seem surprising at first, but it is easily explained: as hydrogen concentration increases, the

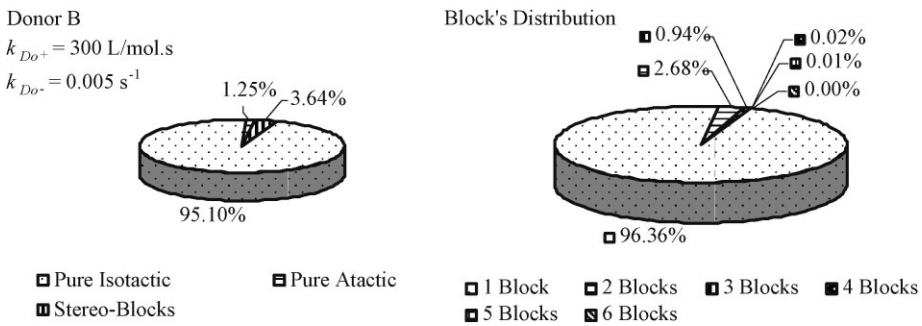

Figure 8.
Better donor type effect at steady state reference polymerization conditions for single site. ($k^+_{Do}(B)/k^+_{Do}$(reference) = 2, $k^-_{Do}(B)/k^-_{Do}$(reference) = 0.5, $k^I_p/k^{II}_p = 1$, $R^I_p/R^I_{tr} = 1364$, and $R^{II}_p/R^{II}_{tr} = 1364$).

Copyright © 2009 WILEY-VCH Verlag GmbH & Co. KGaA, Weinheim

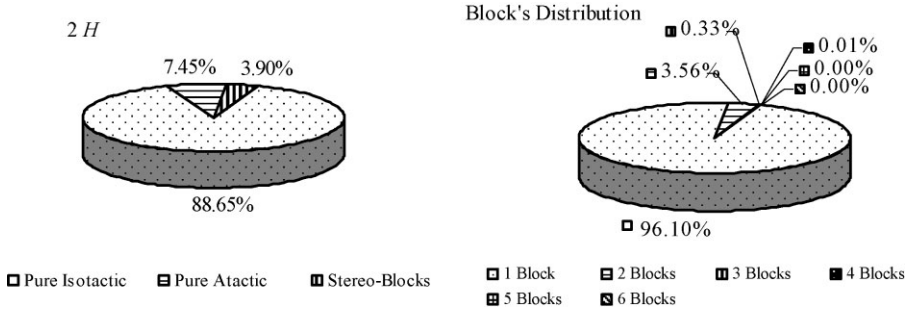

Figure 9.
Doubling hydrogen concentration at steady state reference polymerization conditions for single site. ($M_n = 28{,}600$ g/mol, and $M_w = 57{,}250$ g/mol).

polymer chains become (in average) shorter and, consequently, the likelihood of a change in site state taking place during the lifetime of a polymer chains decreases. Therefore, as the hydrogen concentration increases, the fraction of stereoblock chains decreases, as illustrated in Figure 9.

Due to the presence of more than one active site type in heterogenous Ziegler-Natta catalysts used industrially to polymerize propylene, the model was extended to include multiple site types. The different active sites on heterogeneous Ziegler-Natta catalysts are characterized by distinct polymerization kinetic parameters than can be estimated by MWD deconvolution.[16,17]

Table 8 shows the simulation results for a four-site-type catalyst model. Sites 1 and 2 make only isotactic chains, while Sites 3 and 4 can produce isotactic, atactic and stereoblock chains because they may exist in two states, as described in our proposed mechanism above. Site 1 produces isotactic polypropylene chains with $R_p^I/R_{tr}^I = 1500$ (rate of propagation to rate of termination ratio). However, Site 2 makes chains with longer average molecular weight with $R_p^I/R_{tr}^I = 4000$. Sites 3 and 4 can suffer transformation between stereoselective and non stereoselective states by complexation with an electron donor. Site 3 was assumed to produce around 93 wt% pure isotactic chains, with a ratio of the rate constant of propagation at stereoselective state to the rate constant of propagation of the non stereoselective state of $k_p^I/k_p^{II} = 2.5$

Table 8.
Simulation results for a 4-site model.

Site	Overall		1		2		3		4	
	Mole %	Mass %	Mole %	Mass %	Mole %	Mass %	Mole %	Mass %	Mole %	Mass %
Pure Isotactic	95.13%	98.22%	100.0%	100.0%	100.0%	100.0%	91.16%	93.40%	84.84%	86.47%
Pure Atactic	3.41%	0.30%	0.00%	0.00%	0.00%	0.00%	6.41%	2.84%	6.17%	0.88%
Stereoblocks	1.46%	1.48%	0.00%	0.00%	0.00%	0.00%	2.43%	3.76%	8.99%	12.64%
Block weight %:										
1 block	98.62%	97.98%	100.0%	100.0%	100.0%	100.0%	97.57%	96.24%	91.01%	87.35%
2 blocks	1.12%	1.44%	0.00%	0.00%	0.00%	0.00%	2.22%	3.24%	6.79%	7.89%
3 blocks	0.24%	0.52%	0.00%	0.00%	0.00%	0.00%	0.21%	0.50%	2.00%	4.25%
4 blocks	0.02%	0.04%	0.00%	0.00%	0.00%	0.00%	0.00%	0.01%	0.15%	0.35%
5 blocks	0.00%	0.01%	0.00%	0.00%	0.00%	0.00%	0.00%	0.00%	0.04%	0.14%
6 blocks	0.00%	0.00%	0.00%	0.00%	0.00%	0.00%	0.00%	0.00%	0.00%	0.01%
M_n (g/mol)	52,100		63,000		167,300		7,900		191,500	
M_w (g/mol)	231,500		125,900		334,600		16,000		398,000	
PDI	4.44		2.00		2.00		2.03		2.08	
k_p^I/k_p^{II}							2.50		6.67	
R_p^I/R_{tr}^I			1500		4000		194		5000	
R_p^{II}/R_{tr}^{II}			0		0		97		1071	

Copyright © 2009 WILEY-VCH Verlag GmbH & Co. KGaA, Weinheim

and shorter chains with $R_p^I/R_{tr}^I = 194$ and $R_p^{II}/R_{tr}^{II} = 97$. Site 4 was the least stereoselective site, producing only 86.5 wt % pure isotactic chains with $k_p^I/k_p^{II} = 6.7$ and higher molecular weight averages with $R_p^I/R_{tr}^I = 5000$ and $R_p^{II}/R_{tr}^{II} = 1071$. Table 8 shows that the model can predict the individual properties of polymer made on each site type such as molecular weight averages, polydispersity and molar and mass fractions of each population. The overall properties of the polymer produced by this 4-site catalyst were also predicted where the pure isotactic content was around 98 wt% and with $M_n = 52{,}100$ g/mol, $M_w = 231{,}500$ g/mol, and polydispersity of 4.44. These results are typical of commonly encountered industrial polypropylene resins made with heterogeneous Ziegler-Natta catalysts.

Monte Carlo Simulations

1.1 Using the Monte Carlo algorithm discussed above, it is possible to predict the complete chain length distribution (CLD) of each type of population. For instance, Figure 10 shows the CLDs for all polymer chains, isotactic, atactic, and stereoblock chains, predicted for the polymerization at the reference conditions shown in Table 4 and Table 5. The random noise observed in the CLD is characteristic of Monte Carlo simulations and can be reduced by generating more polymer chains. For the present simulation, over 205,000 polymer chains were generated. This type of detailed microstructural information can only be obtained by the complete solution of the population balances or by Monte Carlo simulation. Monte Carlo simulation is usually much easier to implement, albeit it may require considerable computational time. In the case of the reference electron donor concentration, the mass fraction of isotactic chains was approximately 87.2%, of atactic 5.6%, and of stereoblock 7.2% (the area under the CLDs is proportional to the mass fraction of polymer belonging to that population). The model can also predict number and weight average molecular weights for the overall polymer ($M_n = 57{,}212$ $M_w = 114{,}600$, and $PDI = 2.0$.), isotactic ($M_n = 56{,}819$, $M_w = 113{,}620$, $PDI = 2.0$), atactic ($M_n = 45{,}612$, $M_w = 89{,}699$, $PDI = 2.0$), and stereoblock chains ($M_n =$

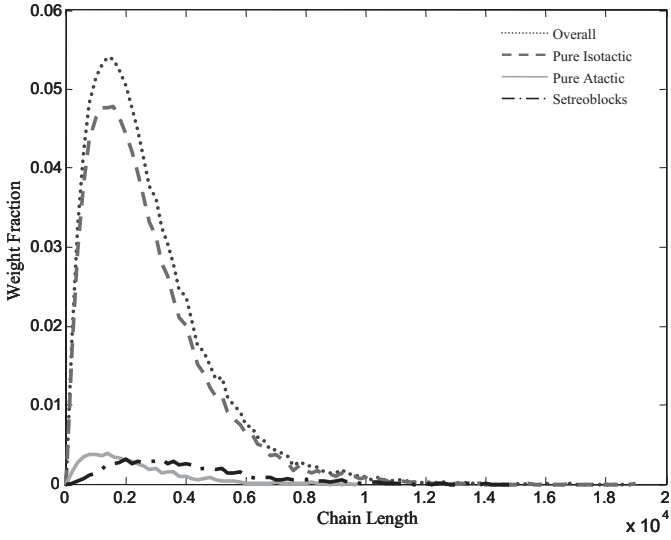

Figure 10.
Monte Carlo simulation of the chain length distributions at reference polymerization conditions; $M_n = 57{,}250$ $M_w = 114{,}600$, $PDI = 2.0$, Isotactic = 87.2%, Atactic = 5.6%, Stereoblocks = 7.2%, and with total number of chains of 205,750.

Copyright © 2009 WILEY-VCH Verlag GmbH & Co. KGaA, Weinheim

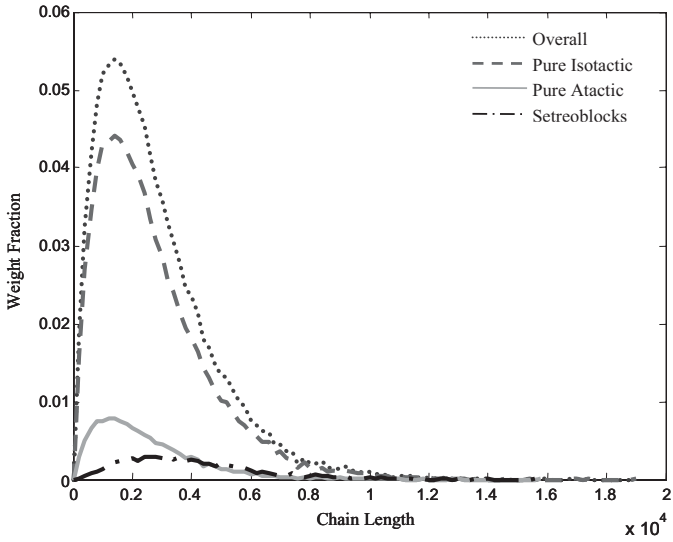

Figure 11.
Monte Carlo simulation of the chain length distributions at ½ × *Do*; $M_n = 57{,}100$ $M_w = 114{,}500$, $PDI = 2.0$, Isotactic = 80.1%, Atactic = 12.9%, Stereoblocks = 7.1%, and with total number of chains of 205,800.

113,780, $M_w = 169{,}830$ and $PDI = 1.5$). The Monte Carlo and method of moments predictions for molecular weights, polydispersities, and the tacticity predictions agree very well proving that both models describe the polymerization adequately.

On the other hand, Figure 11 shows the CLDs predicted when the donor concentration is reduced to half its reference value: the mass fraction of isotactic chains decrease to 80.1%, while that of atactic chains increase to 12.9%, and stereoblock chains have a slight decrease to 7.1%. The number and weight average molecular weights for the overall polymer ($M_n =$ 57,100, $M_w = 114{,}530$, $PDI = 2.0$), isotactic ($M_n = 55{,}820$, $M_w = 111{,}940$, $PDI = 2.0$), atactic ($M_n = 51{,}190$, $M_w = 102{,}250$, $PDI =$ 2.0), and stereoblock chains ($M_n = 110{,}660$, $M_w = 165{,}860$, $PDI = 1.5$) are also easily computed from these simulations.

One of the most common techniques for determining the degree of tacticity in polypropylene is carbon-13 nuclear magnetic resonance (^{13}C NMR). ^{13}C NMR measures the sequence distribution of meso (isotactic, *m*) and racemic (syndiotactic, *r*) placements of the methyl groups along the polymer chain. Sequence distributions up to the pentads were simulated using our Monte Carlo model. Figure 12 illustrates the effect of varying the donor concentration on the pentad sequence of polypropylene. As expected, increasing donor concentration will increase the fraction of *m* placements at the expense of *r* sequences.

The values of the pentad sequence distribution shown in Figure 12 can also be used to back calculate or validate the model accuracy with the values of the tetrad, triad, and dyad sequences using well known mathematical relations between these sequences.[18]

Concluding Remarks

Most commercial heterogeneous Ziegler - Natta catalysts for propylene polymerization have several active site types with varying stereoregular control characteristics that can be affected by the addition of electron donors. Polypropylene chains can be atactic, isotactic, or have an atactic-isotactic stereoblock structure. The stereoblock structure will be produced if the chain starts growing while the site is at the aspecific state and then reacts with an

Copyright © 2009 WILEY-VCH Verlag GmbH & Co. KGaA, Weinheim

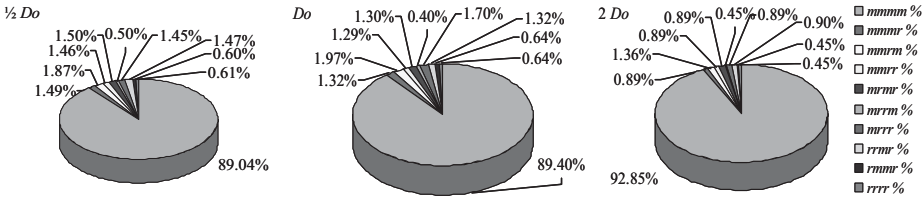

Figure 12.
Pentad sequence distribution.

electron donor molecule and is converted to the stereospecific state before chain termination (or vice-versa). Our model is the first to describe quantitatively this state transformation step during propylene polymerization.

We used the proposed model to show how the several polypropylene chain populations were affected by changing the concentration of hydrogen and electron donor in the reactor during steady-state polymerizations. As expected, molecular weight averages decrease with increasing hydrogen concentration but, more interestingly, hydrogen concentration also affects the fractions of each propylene population. Increasing hydrogen concentration favors the formation of atactic or isotactic chains because it reduces the average lifetime of the polymer chain and decreases the probability of a change in state taking place as the chain grows, forming a stereoblock chain. Moreover, the model shows the effect of the electron donor concentration on polypropylene tacticity. In our simulations, the weight percent of isotactic chains decreases by approximately 6.4% when the donor concentration was reduced by half of its original value. To the best of our knowledge, this is the first time a mathematical model was developed to describe this effect.

In addition, our model gives a detailed description of the different polypropylene populations. The polydispersity of the purely atactic or isotactic chains is equal to 2.0, but the *PDI* decreases as the number of stereoblocks increases due to the statistical averaging of the chain lengths. The molecular weight averages increase with increasing number of blocks, as expected. The model is also capable to predict the mole and mass fraction of each polymer species in the mixture.

Typical heterogeneous Zigler-Natta catalysts used for propylene polymerization have two or more site types. These catalysts can be modeled with the same approach described above, provided that each site type is described with a different set of polymerization kinetic parameters. Therefore, both steady-state and dynamic simulations for a 4-site type catalyst were carried out where sites type 1 and 2 make only isotactic chains and sites type 3 and 4 alternate between aspecific and stereospecific states. The polydispersity of chains made on each site type is still equal to 2.0, but the overall polydispersity of the polymer was 4.45. Moreover, illustration of how varying the donor concentration affects the mass fraction of atactic and isotactic chains in the reactor was reported.

The model using the method of moments can follow molecular weight averages, but not the complete molecular weight distribution. Monte Carlo simulation was used to predict the complete MWD and tacticity sequence length distribution.

[1] V. Buscio, R. Cipullo, *Prog. Polym. Sci.* **2001**, *26*, 443.
[2] F. Shimizu, J. T. M. Pater, G. Weickert, *J. Appl. Polym. Sci.* **2001**, *81*, 1035.
[3] J. C. Chadwick, G. M. M. van Kessel, O. Sudmeijer, *Macromol. Chem. Phys.* **1995**, *196*, 1431.
[4] W. H. Ray, J. B. P. Soares, R. A. Hutchinson, *Macrimol. Symp.* **2004**, *206*, 1.
[5] M. C. Forte, F. M. B. Coutinho, *Eur. Polym. J.* **1996**, *32*, No. 5, 605.
[6] M. Kakugo, T. Miyatake, Y. Naito, K. Mizunuma, *Macromolecules*, **1988**, *21*, 314.
[7] V. Busico, R. Cipullo, P. Corradini, R. De Biasio, *Macromol. Chem. Phys.* **1995**, *196*, 491.

Copyright © 2009 WILEY-VCH Verlag GmbH & Co. KGaA, Weinheim

[8] V. Busico, R. Cipullo, G. Monaco, G. Talarico, J. C. Chadwick, A. L. Segre, O. Sudmeijer, *Macromolecules*, **1999**, *32*, 4173.
[9] A. Alshaiban, **2008**, MASc. Thesis, University of Waterloo.
[10] P. Canu, W. H. Ray, *Comp. Chem. Eng.* **1991**, *15*, 549–564.
[11] W. H. Ray, *J. Macromol. Sci., Rev. Macromol. Chem.*, **1972**, *C8*, 1–56.
[12] J. B. P. Soares, A. E. Hamielec, *Polym React Eng*, **1996**, *4*, 153–191.
[13] L. C. Simon, J. B. P. Soares, *Macromol. Theory Simul.*, **2002**, *11*, 222.
[14] M. C. Haag, L. C. Simon, J. B. P. Soares, *Macromol. Theory. Simul.* **2003**, *12*, 142.
[15] D. Beigzadeh, J. B. P. Soares, T. A. Duever, *J. Appl. Polym. Sci.* **2001**, *80*, 2200.
[16] A. Faldi, J. B. P. Soares, *Polymer*, **2004**, *42*, 3057.
[17] J. B. P. Soares, A. E. Hamielec, *Polymer*, **1995**, *36*, 2257.
[18] G. Odian, "*Principles of Polymerization*", 4th ed., J. Wiley & Sons, **2004**.

Appendix A

Dynamic population balance equations are shown in Tables A-1 to A-3. The full derivation of these equations was given by Alshaiban.[9]

Table A-1.
Population balance for the overall, pure, and stereoblock chains.

Overall			
(A1)	$\frac{dP_0^I}{dt} = k_a^I C_I Al + k_{Do}^+ Do P_0^{II} - (k_i^I M + k_{Do}^- + K_{D1} + s) P_0^I$	(A2)	$\frac{dD_r^I}{dt} = (K_{T1} + K_{D1}) P_r^I - s D_r^I$
(A3)	$\frac{dP_0^{II}}{dt} = k_a^{II} C_{II} Al + k_{Do}^- P_0^I - (k_i^{II} M + k_{Do}^+ Do + K_{D2} + s) P_0^{II}$	(A4)	$\frac{dD_r^{II}}{dt} = (K_{T2} + K_{D2}) P_r^{II} - s D_r^{II}$
(A5)	$\frac{dP_1^I}{dt} = (k_i^I P_0^I + k_{iH}^I P_H^I + k_{iR}^I P_{Et}^I) M + k_M^I M \sum_{r=1}^{\infty} P_r^I + k_{Do}^+ Do P_1^{II} - k_p^I M P_1^I - (k_{Do}^- + K_{T1} + K_{D1} + s) P_1^I$		
(A6)	$\frac{dP_r^I}{dt} = k_p^I M P_{r-1}^I + k_{Do}^+ Do P_r^{II} - k_p^I M P_r^I - (k_{Do}^- + K_{T1} + K_{D1} + s) P_r^I$		
(A7)	$\frac{dP_1^{II}}{dt} = (k_i^{II} P_0^{II} + k_{iH}^{II} P_H^{II} + k_{iR}^{II} P_{Et}^{II}) M + k_M^{II} M \sum_{r=1}^{\infty} P_r^{II} + k_{Do}^- P_1^I - k_p^{II} M P_1^{II} - (k_{Do}^+ Do + K_{T2} + K_{D2} + s) P_1^{II}$		
(A8)	$\frac{dP_r^{II}}{dt} = k_p^{II} M P_{r-1}^{II} + k_{Do}^- P_r^I - k_p^{II} M P_r^{II} - (k_{Do}^+ Do + K_{T2} + K_{D2} + s) P_r^{II}$		
Pure Chains			
(A9)	$\frac{dP_{1,1}^I}{dt} = (k_i^I P_0^I + k_{iH}^I P_H^I + k_{iR}^I P_{Et}^I) M + k_M^I M \sum_{r=1}^{\infty} P_r^I - k_p^I M P_{1,1}^I - (k_{Do}^- + K_{T1} + K_{D1} + s) P_{1,1}^I$		
(A10)	$\frac{dP_{r,1}^I}{dt} = k_p^I M (P_{r-1,1}^I - P_{r,1}^I) - (k_{Do}^- + K_{T1} + K_{D1} + s) P_{r,1}^I$	(A11)	$\frac{dD_{r,1}^I}{dt} = (K_{T1} + K_{D1}) P_{r,1}^I - s D_{r,1}^I$
(A12)	$\frac{dP_{1,1}^{II}}{dt} = (k_i^{II} P_0^{II} + k_{iH}^{II} P_H^{II} + k_{iR}^{II} P_{Et}^{II}) M + k_M^{II} M \sum_{r=1}^{\infty} P_r^{II} - k_p^{II} M P_{1,1}^{II} - (k_{Do}^+ Do + K_{T2} + K_{D2} + s) P_{1,1}^{II}$		
(A13)	$\frac{dP_{r,1}^{II}}{dt} = k_p^{II} M (P_{r-1,1}^{II} - P_{r,1}^{II}) - (k_{Do}^+ Do + K_{T2} + K_{D2} + s) P_{r,1}^{II}$	(A14)	$\frac{dD_{r,1}^{II}}{dt} = (K_{T1} + K_{D1}) P_{r,1}^{II} - s D_{r,1}^{II}$
Stereoblocks			
(A15)	$\frac{dP_{r,i}^I}{dt} = k_{p1} M (P_{r-1,i}^I - P_{r,i}^I) + k_{Do}^+ Do P_{r,i-1}^{II} - (k_{Do}^- + K_{T1} + K_{D1} + s) P_{r,i}^I$	(A16)	$\frac{dD_{r,i}^I}{dt} = (K_{T1} + K_{D1}) P_{r,i}^I - s D_{r,i}^I$
(A16)	$\frac{dP_{r,i}^{II}}{dt} = k_{p2} M (P_{r-1,i}^{II} - P_{r,i}^{II}) + k_{Do}^- P_{r,i-1}^I - (k_{Do}^+ Do + K_{T2} + K_{D2} + s) P_{r,i}^{II}$	(A17)	$\frac{dD_{r,i}^{II}}{dt} = (K_{T1} + K_{D1}) P_{r,i}^{II} - s D_{r,i}^{II}$

Table A-2.
Population balance for the chain segments.

Equation	
(A18)	$\frac{dB_0^I}{dt} = k_a^I Al C_I + k_{Do}^+ Do B_0^{II} + k_{Do}^+ Do \sum_{r=1}^{\infty} B_r^{II} + K'_{T1} \sum_{r=1}^{\infty} B_r^I - k_i^I M B_0^I - (k_{Do}^- + K_{D1} + s) B_0^I$
(A19)	$\frac{dB_1^I}{dt} = k_i^I M B_0^I - k_p^I M B_1^I - (k_{Do}^- + K'_{T1} + K_{D1} + s) B_1^I$
(A20)	$\frac{dB_r^I}{dt} = k_p^I M (B_{r-1}^I - B_r^I) - (k_{Do}^- + K_{T1} + K_{D1} + s) B_r^I$
(A21)	$\frac{dB_0^{II}}{dt} = k_a^{II} Al C_{II} + k_{Do}^- B_0^I + k_{Do}^- \sum_{r=1}^{\infty} B_r^I + K'_{T2} \sum_{r=1}^{\infty} B_r^{II} - k_i^{II} M B_0^{II} - (k_{Do}^+ Do + K_{D2} + s) B_0^{II}$
(A22)	$\frac{dB_1^{II}}{dt} = k_i^{II} M B_0^{II} - k_p^{II} M B_1^{II} - (k_{Do}^+ Do + K'_{T1} + K_{D1} + s) B_1^{II}$
(A23)	$\frac{dB_r^{II}}{dt} = k_p^{II} M (B_{r-1}^{II} - B_r^{II}) - (k_{Do}^+ Do + K_{T1} + K_{D1} + s) B_r^{II}$

Copyright © 2009 WILEY-VCH Verlag GmbH & Co. KGaA, Weinheim

Table A-3.
Other steady-state equations and definitions

No.	Equation	No.	Equation	No.	Equation
(A24)	$P_0^I = \frac{K_{A1}C_I + k_{Do}^+ Do P_0^{II}}{k_i^I M + \alpha_1}$	(A25)	$K_{A1} = k_{a1}Al$	(A26)	$\delta_1 = \frac{k_p^I}{k_{Do}^- + K_{T1} + K_{D1} + s}$
(A27)	$P_0^{II} = \frac{K_{A2}C_{II} + k_{Do}^- P_0^I}{k_i^{II} M + \alpha_2}$	(A28)	$K_{A2} = k_{a2}Al$	(A29)	$\delta_1' = \frac{k_p^I}{k_{Do}^- + K_{T1}' + K_{D1} + s}$
(A30)	$P_H^I = \frac{(k_\beta^I + k_H^I H) Y_I^0 + k_{Do}^+ Do P_H^{II}}{k_{iH}^I M + \alpha_1}$	(A31)	$K_{T1}' = k_\beta^I + k_H^I H + k_{Al}^I Al$	(A32)	$\delta_1'' = \frac{k_M^I}{k_{Do}^- + K_{T1} + K_{D1} + s}$
(A33)	$P_H^{II} = \frac{(k_\beta^{II} + k_H^{II} H) Y_{II}^0 + k_{Do}^- P_H^I}{k_{iH}^{II} M + \alpha_2}$	(A34)	$K_{D1} = k_d^I + k_{d\cdot I}^I I$	(A35)	$\delta_2 = \frac{k_p^{II}}{k_{Do}^+ Do + K_{T2} + K_{D2} + s}$
(A36)	$P_{Et}^I = \frac{k_{Al}^I Al Y_I^0 + k_{Do}^+ Do P_{Et}^{II}}{k_{iR}^I M + \alpha_1}$	(A37)	$K_{T2}' = k_\beta^{II} + k_H^{II} H + k_{Al}^{II} Al$	(A38)	$\delta_2' = \frac{k_p^{II}}{k_{Do}^+ Do + K_{T2}' + K_{D2} + s}$
(A39)	$P_{Et}^{II} = \frac{k_{Al}^{II} Al Y_{II}^0 + k_{Do}^- P_{Et}^I}{k_{iR}^{II} M + \alpha_2}$	(A40)	$K_{D2} = k_d^{II} + k_{d\cdot I}^{II} I$	(A41)	$\delta_2'' = \frac{k_M^{II}}{k_{Do}^+ Do + K_{T2}' + K_{D2} + s}$
(A42)	$B_0^I = \frac{K_{A1}C_I + k_{Do}^- Do B_0^{II} + k_{Do}^+ Do W_{II}^0 + K_{T1}' W_I^0}{k_i^I M + \alpha_1}$	(A43)	$\alpha_1 = k_{Do}^- + K_{D1} + s$	(A44)	$\gamma_1 = \frac{(k_i^I P_0^I + k_{iH}^I P_H^I + k_{iR}^I P_{Et}^I)}{(k_{Do}^- + K_{T1} + K_{D1} + s)}$
(A45)	$B_0^{II} = \frac{K_{A2}C_{II} + k_{Do}^- B_0^I + k_{Do}^- W_I^0 + K_{T2}' W_{II}^0}{k_i^{II} M + \alpha_2}$	(A46)	$\alpha_2 = k_{Do}^+ Do + K_{D2} + s$	(A47)	$\gamma_1' = \frac{k_i^I P_0^I + k_{iH}^I P_H^I + k_{iR}^I P_{Et}^I}{k_{Do}^- + K_{T1}' + K_{D1} + s}$
(A48)	$B_1^I = \frac{k_{h1} M B_0^I}{k_p^I M + k_{Do}^- + K_{T1}' + K_{D1} + s}$	(A49)	$\beta_1 = \frac{k_{Do}^+ Do}{k_{Do}^- + K_{T1} + K_{D1} + s}$	(50)	$\gamma_1'' = \frac{k_i^I B_0^I + k_M^I B_1^I}{k_{Do}^- + K_{T1} + K_{D1} + s}$
(A51)	$B_1^{II} = \frac{k_{I2} M B_0^{II}}{k_p^{II} M B_1^{II} + k_{Do}^+ Do + K_{T1}' + K_{D1} + s}$	(A52)	$\beta_1' = \frac{k_{Do}^+ Do}{k_{Do}^- + K_{T1}' + K_{D1} + s}$	(A53)	$\gamma_2 = \frac{k_i^{II} P_0^{II} + k_{iH}^{II} P_H^{II} + k_{iR}^{II} P_{Et}^{II}}{k_{Do}^+ Do + K_{T2} + K_{D2} + s}$
(A54)	$K_{T1} = k_\beta^I + k_M^I M + k_H^I H + k_{Al}^I Al$	(A55)	$\beta_2 = \frac{k_{Do}^-}{k_{Do}^+ Do + K_{T2} + K_{D2} + s}$	(A56)	$\gamma_2' = \frac{k_i^{II} P_0^{II} + k_{iH}^{II} P_H^{II} + k_{iR}^{II} P_{Et}^{II}}{k_{Do}^+ Do + K_{T2}' + K_{D2} + s}$
(A57)	$K_{T2} = k_\beta^{II} + k_M^{II} M + k_H^{II} H + k_{Al}^{II} Al$	(A58)	$\beta_2' = \frac{k_{Do}^-}{k_{Do}^+ Do + K_{T2}' + K_{D2} + s}$	(A59)	$\gamma_2'' = \frac{k_i^{II} B_0^{II} + k_M^{II} B_1^{II}}{k_{Do}^+ Do + K_{T2} + K_{D2} + s}$

Copyright © 2009 WILEY-VCH Verlag GmbH & Co. KGaA, Weinheim